

Isolation and identification of leukocyte populations in intracranial blood collected during mechanical thrombectomy

Journal of Cerebral Blood Flow & Metabolism
2022, Vol. 42(2) 280–291
© The Author(s) 2021



Article reuse guidelines:
sagepub.com/journals-permissions
DOI: 10.1177/0271678X211028496
journals.sagepub.com/home/jcbfm



Benjamin C Shaw¹ , G Benton Maglinger², Thomas Ujas²,
Chintan Rupareliya^{3,4}, Justin F Fraser^{3,4,5,6},
Stephen Grupke^{3,5} , Melissa Kesler⁷, Mathias Gelderblom⁸,
Keith R Pennypacker^{2,4,6}, Jadwiga Turchan-Cholewo^{1,6} and
Ann M Stowe^{1,2,4,6} 

Abstract

Using standard techniques during mechanical thrombectomy, the Blood and Clot Thrombectomy Registry and Collaboration (BACTRAC) protocol (NCT03153683) isolates intracranial arterial blood distal to the thrombus and proximal systemic blood in the carotid artery. We augmented the current protocol to study leukocyte subpopulations both distal and proximal to the thrombus during human stroke ($n = 16$ patients), and from patients with cerebrovascular disease (CVD) undergoing angiography for unrelated conditions (e.g. carotid artery stenosis; $n = 12$ patients). We isolated leukocytes for flow cytometry from small volume (< 1 mL) intracranial blood and systemic blood (5–10 mL) to identify adaptive and innate leukocyte populations, in addition to platelets and endothelial cells (ECs). Intracranial blood exhibited significant increases in T cell representation and decreases in myeloid/macrophage representation compared to within-patient carotid artery samples. $CD4^+$ T cells and classical dendritic cells were significantly lower than CVD controls and correlated to within-patient edema volume and last known normal. This novel protocol successfully isolates leukocytes from small volume intracranial blood samples of stroke patients at time of mechanical thrombectomy and can be used to confirm preclinical results, as well as identify novel targets for immunotherapies.

Keywords

Cerebrovascular endothelium, emergent large vessel occlusion (ELVO), flow cytometry, ischemic stroke, T cells

Received 22 July 2020; Revised 31 May 2021; Accepted 2 June 2021

Introduction

Since 2015, mechanical thrombectomy has become the standard treatment for emergent large vessel occlusion (ELVO) ischemic stroke.^{1–7} ELVOs are the most devastating acute blockages of cerebral vessels and can represent 30–40% of ischemic strokes.⁸ Randomized clinical trials demonstrate the superiority of mechanical thrombectomy over fibrinolytic medical management alone, and continue to expand the inclusion criteria for this treatment. Since mechanical thrombectomy has become a standard of care, research has aimed at investigating the tissue obtained from this procedure, specifically thrombus morphology and composition,

¹Sanders-Brown Center on Aging, University of Kentucky, Lexington, USA

²Department of Neurology, University of Kentucky, Lexington, USA

³Department of Neurosurgery, University of Kentucky, Lexington, USA

⁴Center for Advanced Translational Stroke Science, University of Kentucky, Lexington, USA

⁵Department of Radiology, University of Kentucky, Lexington, USA

⁶Department of Neuroscience, University of Kentucky, Lexington, USA

⁷Department of Pathology and Laboratory Medicine, University of Kentucky, Lexington, USA

⁸Department of Neurology, University Hospital Hamburg Eppendorf, Hamburg, Germany

Corresponding author:

Ann M Stowe, Department of Neurology, BBSRB 379, 741 S. Limestone St., Lexington, KY 40508, USA.

Email: ann.stowe@uky.edu

including proportions of fibrin/platelets and white blood cells/red blood cells.^{9–15}

Our institution began translationally utilizing thrombectomy as an opportunity to learn more about acute ischemic stroke pathology. The Blood and Clot Thrombectomy Registry and Collaboration (BACTRAC) protocol (clinicaltrials.gov NCT03153683) now represents one of the only prospective, continually enrolling tissue banks of its kind.¹⁶ Using the standard techniques entailed in mechanical thrombectomy, BACTRAC isolates intracranial blood within the artery immediately downstream from the thrombus, systemic carotid arterial blood proximal to the thrombus, and the thrombus itself. These samples provide novel insight into the molecular and cellular changes that occur within the area of infarction. To date, BACTRAC samples identified within-patient acid-base changes, electrolyte chemistry, and changes in gene and protein expression in intracranial blood with systemic blood as internal comparative controls.^{17–20}

In this study, we set out to investigate how neuro-inflammatory responses relate to these previous findings. We started with the established BACTRAC protocol and further developed this protocol to isolate leukocytes for flow cytometry. In addition to leukocyte isolation, this revised protocol allowed for banking of thrombus and plasma for subsequent histopathological and proteomic analyses. We developed a flow cytometry panel that identifies B cells, T cells, dendritic cells, NK cells, macrophages, monocytes, granulocytes, platelets, and endothelial cells. Based on our preliminary results, standard-of-care interventional techniques at any institution may be used to collect intracranial blood to facilitate studies investigating the pathophysiology of acute ischemic neuroinflammatory mechanisms.

Methods

Subjects: All subjects and/or their study partners signed the written informed consent approved by the Institutional Review Board of the University of Kentucky, in accordance with the Federal-wide Assurance on file with the Department of Health and Human Services (USA). Twenty-two ischemic stroke patients aged 49 to 89 years participated in this study (Table 1). Time between last known normal (LKN) and sample collection during angioplasty ranged from 2.7 to 27.8 hours (11.5 ± 6.6 hrs). Intracranial blood is always taken immediately after the microcatheter is navigated distal to the thrombus and before first pass. Therefore, the thrombectomy device used does not affect intracranial sampling as the sample is taken prior to initiation of thrombectomy. Subjects were screened *post hoc* for medical or pharmacological confounds and relevant comorbidities. Four patients were

Table 1. Patient demographics (editable format).

	Value (%)
Age (median; range)	73 (49–89)
Sex	
Female	9 (56)
Male	7 (44)
BMI	
Unreported	1
<24.9	2 (13)
25–29.9	6 (38)
30–39.9	5 (31)
>40	2 (13)
Comorbidities	
Hypertension	13 (81)
Diabetes Mellitus II	7 (44)
Hyperlipidemia	3 (19)
Previous Stroke	4 (25)
Previous MI	1 (6)
NIHSS on admission	
Minor Stroke (1–4)	0 (0)
Moderate Stroke (5–15)	8 (50)
Moderate/Severe (16–20)	6 (38)
Severe Stroke (≥ 21)	2 (13)
TICI score	
2A = <50% Perfusion	1 (6)
2B = >50% Perfusion	5 (31)
3 = Full Perfusion	10 (63)
LKN to Thrombectomy	690 min (159–1665 min)
Completion time (mean; range)	1 unreported
Infarct Volume (mean \pm SD)	103,254.9 \pm 134,816.2 mm ³
	2 unreported
CTA colateral score	
Unreported	3 (19)
0	5 (31)
1	7 (44)
2	0 (0)
3	0 (0)
4	1 (6)

excluded from analysis *post hoc* due to aberrant auto-fluorescence in samples, and two samples were too small in volume and cell count for analysis, resulting in sixteen patients included in the final analysis. Twelve patients undergoing angiography for conditions other than stroke (i.e. carotid artery stenosis) also consented to provide cerebral arterial blood samples which were used as the control population (aged 28–76 years). Twelve healthy volunteer donors ranging from 25 to 63 years (6 male, 8 female) provided venous blood samples for comparison by antecubital venipuncture.

Optimization of leukocyte isolation protocol for intracranial blood: Our isolation protocols were optimized first using volunteer peripheral venous blood samples. From their samples, 1 ml of blood was treated as a mock ‘intracranial’ sample of a stroke patient and 9 ml was treated as the systemic sample from a stroke

patient. The viability and yield of 1 mL and 9 mL samples were assessed after processing to ensure comparable survival and yield per volume.

Blood collection and cryopreservation: Workflow of sample collection and processing can be found in Supplemental Figure 1. Tissue samples are obtained from the angiography suite at the time of thrombectomy for each subject. Blood samples are transported at room temperature and then placed on a rocker until processing. Both intracranial and systemic blood samples were spun down at $515 \times g$ for 10 minutes at 27°C . One 200 μL aliquot of intracranial blood plasma and eleven 200 μL aliquots of systemic blood plasma are cooled to -80°C at $1^\circ\text{C}/\text{min}$ and banked. The intracranial blood pellet was resuspended to a final volume of 4 mL with PBS, and the systemic blood pellet was resuspended to a final volume of 20 mL with PBS. Both samples were then layered over an equal volume of Ficoll and spun at $400 g$ for 30 minutes at room temperature. After centrifugation, the buffy coats were removed and samples resuspended in PBS (systemic to 45 mL, intracranial to 14 mL). Tubes were then spun at $450 \times g$ for 10 minutes at 4°C . After centrifugation, samples were decanted, resuspended in either 0.5 (intracranial) or 5.0 mL (systemic) PBS, and triturated for counting. The pellet is first resuspended in Cryopreservation Medium A, and then Cryopreservation Medium B (composition found in Supplemental Table 1) is added to approximately 20,000 cells/ml when possible. Samples were placed in cryovials and cooled to -80°C at $1^\circ\text{C}/\text{min}$ then transferred to liquid nitrogen for long-term storage.

Recovery from Cryopreservation and Flow Cytometry: Samples were thawed from cryopreservation media at 37°C for 2 min. Cells were counted using Nexcelom Cellometer and ViaStain AOPI dye #CS2-0106. Samples were split for separate panel staining, with at least 1×10^6 cells from healthy volunteer and systemic blood or 2×10^5 cells for intracranial blood aliquoted for the General Immunophenotyping Panel, and the remainder for the Supplemental Panel. Antibody staining and preparation was performed as previously described.²¹ Briefly, cells were washed once in PBS and incubated in Ghost Dye 780 (Tonbo Biosciences) with PBS on ice in the dark for 30 minutes. Cells were then washed twice in FACS buffer (PBS, 1% bovine serum albumin, 0.01% sodium azide) and blocked using human FcR blocking reagent (Mitenyi Biotec #130-059-901) for 5 minutes at room temperature. Antibodies were added without washing and incubated on ice for 30 minutes in the dark. Cells were washed twice in FACS buffer and fixed in 1% paraformaldehyde plus 0.1% EDTA on ice for 30 minutes then analyzed on a FACSymphony (BD Biosciences) the same day. Channel voltages were assigned with volunteer samples and compensation calculated using

UltraComp beads (Invitrogen, # 01-2222-42) and heat killed (65°C , 1 minute) cells for viability stain. All channels were acquired, including channels without an assigned dye, to aid compensation; FSC-H was also acquired to gate on singlet events. Compensation calculation was performed through FlowJo V10 (TreeStar), treated as spectral with weights for unused channels optimized. Volunteer and systemic blood sample acquisition included 500,000 events, while the intracranial blood sample acquisition included 10,000 events. Intracranial samples with fewer than 10,000 cells were collected in their entirety. Antibody clones, conjugates, vendors, and dilutions are detailed in Supplemental Table 2. Importantly, the cryopreservation and recovery processes did not affect antigen integrity, as there were no reductions in fluorescence intensity after thawing (Supplemental Figure 2).

Gating Strategy: All gating and event analyses were performed in FlowJo V10 (TreeStar). Two panels were used in the analysis: the larger General Immunophenotyping Panel (GIP) and a smaller Supplementary Panel (SP). The GIP (Supplemental Table 2) contained a viability stain (Ghost Dye 780), pan-leukocyte marker (CD45), T cell markers (CD3, CD4, CD8), B cell marker (CD19), myeloid markers (CD11b, CD14), NK cell marker (NK1.1), granulocyte marker (CD66b), and dendritic cell marker (CD11c). Further phenotyping markers included CXCR3 and CD138 to identify effector T cells and plasma cells, respectively. The SP (Supplemental Table 2) contained the same viability stain and CD45 antibody, along with a platelet marker (CD41a) and endothelial cell marker (CD31). Data collected were cleaned before analysis using the FlowAI plugin to remove statistically aberrant data points due to power fluctuations and random noise over time.²² A detailed graphical representation of the overall gating strategy is shown in Supplemental Figure 3. Briefly, $\text{CD41a}^+ \text{CD45}^- \text{FSC-A}^{\text{low}}$ events were classified as platelets using SP, and a generalized FSC-A SSC-A gate defined to exclude these events. This platelet exclusion gate was then applied to all GIP samples. Doublets were excluded using FSC-A FSC-H gating, and leukocytes gated by $\text{CD45}^+ \text{FSC-A}$. Samples with at least 2000 events were downsampled using the Downsample plugin, concatenated into a single file, and reduced to a two dimensional plot using *t*-distributed Stochastic Neighbor Embedding (tSNE). Manual gates for lineage markers were defined using histograms and overlaid to the tSNE plot for confirmation of gating specificity, with additional gating performed if a manual gate encompassed at least two populations on the tSNE plot or until manual gating did not refine the populations further. The remaining unidentified populations were defined by considering their total expression profiles.

For the SP, platelets were defined as described above and the endothelial cell gate defined as CD31⁺ CD45⁻. Distribution profiles (i.e. linear vs. non-linear) were analyzed to determine normality of distribution for appropriate statistical analyses. Of the adaptive immune cell populations, CD19⁺ B cells failed to meet normal distribution within both healthy venous blood samples and intracranial stroke samples, and total T cells failed in the cerebrovascular disease (CVD) control group. Of the innate subsets, granulocytes in healthy control, classical dendritic cells in both stroke samples, myeloid-derived dendritic cells and monocytes in intracranial samples and NK cells failed normality tests.

Granulocyte staining and quantification: Sections of 4 μm thickness were prepared and dried at 58°C for a minimum of 1 hour. Slides were deparaffinized in 2 changes of xylene, hydrated stepwise through ethanol to water, stained in Harris' hematoxylin for 7 minutes followed by a dip in acid ethanol and bluing in ammonia water. Slides were subsequently stained for 3 minutes in eosin before dehydrating stepwise, clearing in xylene, and mounting with Cytoseal. Slides were imaged at 40X, and neutrophils manually counted by a blind observer. Four fields were counted for each thrombus and averaged.

Statistical Analyses: Statistical analyses were performed in GraphPad Prism 8. All data sets were tested for normal distribution using D'Agostino & Pearson test. Comparisons of leukocyte populations between systemic and intracranial blood from patients relied on a paired Student's t test, or a Wilcoxon matched-pairs ranked sign test in the case of non-normally distributed data. Populations between stroke patients and CVD controls were compared by one-way ANOVA. Lymphocyte yield was compared using a two-way ANOVA followed by Tukey post-hoc correction for multiple comparisons. Endothelial cell populations, platelet populations, and leukocyte viability before and after cryopreservation were compared using Residual Maximum Likelihood (REML) linear mixed model with Tukey post-hoc correction for multiple comparisons. Finally, intracranial and systemic populations were compared to patient demographics (BMI, NIHSS, time from LKN, infarct volume, and edema volume) by Spearman non-parametric correlation.

Results

Patient Characteristics: Subject demographics are shown in Table 1. There were 16 adult subjects included in the study with a median age of 73 (49–89), of which 9 (56%) were female. Two subjects had a normal body mass index (BMI), 6 were overweight,

and 7 were obese (one patient's data not reported in medical record). Thirteen subjects had hypertension, 7 had type II diabetes mellitus, 3 had hyperlipidemia, 4 had a history of a previous stroke, and 1 had a previous myocardial infarction. Three were current smokers, 6 never smoked, and the rest did not answer. Five were administered tissue plasminogen activator prior to thrombectomy. According to the National Institutes of Health Stroke Score (NIHSS), on admission 8 subjects had a moderate stroke (NIHSS 5–15), 6 had a moderate/severe stroke (NIHSS 16–20), and 2 had a severe stroke (NIHSS ≥21). The mean LKN to thrombectomy completion time was 690 ± 393 minutes (one patient's data not reported by physician).

Lymphocyte Isolation: Normalized lymphocyte yield and lymphocyte viability are depicted in Figure 1(a). From 10 healthy controls, the average lymphocyte isolation from the 1 mL specimen (i.e. simulated volume of intracranial blood) was 2.13 ± 0.69 × 10⁶ cells/mL. The average lymphocyte isolation from the 9 mL specimen (i.e. simulated volume of systemic blood) was 2.15 ± 0.53 × 10⁶ cells/mL. The average intracranial lymphocyte yield was 1.90 ± 1.11 × 10⁶ cells/mL and the average systemic blood yield was 2.28 ± 0.71 × 10⁶ cells/mL. Repeated measures two-way ANOVA demonstrates that processing smaller volumes of intracranial blood has no effect on leukocyte yield for all populations ($F_{1,44} = 0.67$, $p = 0.42$ for volume; $F_{1,44} = 0.04$, $p = 0.84$ for injury status), though intracranial stroke samples did exhibit a wider distribution of yield. Surprisingly, intracranial blood samples did not have compromised viability compared to systemic stroke samples or volunteer peripheral samples at the time of cryopreservation ($F_{2,26} = 0.07$, $p = 0.93$; Figure 1(b)). There was, however, significant loss of cell viability after recovery among all groups (95.8% vs. 64.3%; $F_{1,15} = 235.9$, $p < 0.0001$). This loss of viability was not restricted to a certain group; the intracranial, systemic, and healthy and cerebrovascular control peripheral samples experienced comparable losses in viability and were not significantly different from each other (Figure 1(b)). Finally, the length of time from LKN to mechanical thrombectomy did not affect intracranial cell viability at time of collection ($F_{1,11} = 1.81$, $p = 0.21$; Figure 1(c)).

Identification of leukocyte populations from stroke patients and controls: Flow cytometry data generated was analyzed and the tSNE algorithm applied on live, CD45⁺ events to aid in cell population identification (Figure 2(a)). Gates were successively applied to delineate populations until only a single population was observed in the tSNE plot. All populations as a percent of CD45⁺ cells are detailed in Table 2, and gates used to define general immune cell types provided in Supplemental Figures 4 to 8. In thrombectomy patients, the systemic blood profiles differ greatly

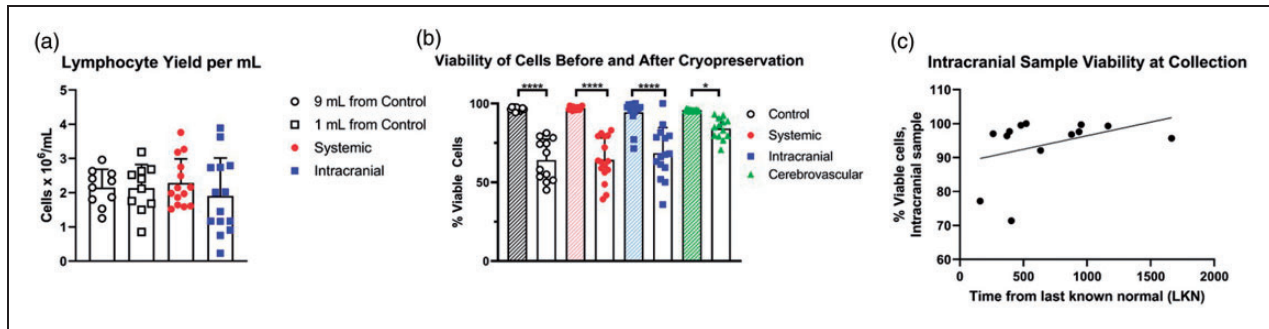


Figure 1. Cell yield and viability. (a) Viability of cells is independent of volume processed for 1 mL volumes (squares) and 9 mL volumes (circles). $F_{1,44} = 0.67$, $p = 0.42$ for volume; $F_{1,44} = 0.04$, $p = 0.84$ for injury status; $n = 10$ controls (white symbols); $n = 14$ stroke patients (red/blue symbols). (b) Significant viability loss occurred during the cryopreservation process (clear bars) compared to viability prior to banking (hatched bars). * $p < 0.05$; **** $p < 0.0001$; $n = 12$ controls (clear circles), $n = 16$ stroke (filled circles, systemic; squares, intracranial), $n = 12$ cerebrovascular disease patients (triangles). One intracranial sample was unreadable using the Nexcelom Cellometer after recovery from cryopreservation but did have viable cells by flow cytometry. (c) Correlation between last known normal and % viability in intracranial blood at time of collection does not show an effect of time to mechanical thrombectomy on leukocyte yield; $F_{1,11} = 1.81$, $p = 0.21$. $r^2 = 0.14$.

versus within-patient intracranial blood, resulting in expression patterns of circulating leukocytes that more closely resemble those of healthy controls (Figure 2(c), (e)), while the intracranial samples more closely resemble the CVD controls (Figure 2(d), (f)).

Ischemic stroke shifts cell populations in intracranial vs. systemic blood: Figure 3 shows the results for leukocyte representation in arterial samples from CVD patients compared to systemic and intracranial blood from thrombectomy patients. Analysis of leukocyte populations within each stroke patient uncovered an overrepresentation of $CD3^+$ T cells in the intracranial blood ($p = 0.01$; Figure 3(b)). Both $CD4^+$ T cell ($p = 0.02$) and $CD8^+$ T cell ($p = 0.02$) subpopulations were also significantly increased in the intracranial blood. Interestingly, both intracranial and systemic $CD4^+$ T cells were significantly lower than the CVD patient controls ($p < 0.01$). Total T cells were also significantly lower in the systemic, but not intracranial, samples compared to CVD patient controls ($p = 0.05$). Additionally, a subset of NK T cells ($CD161^+CD3^+CD4^+$) were significantly increased in the intracranial blood ($p = 0.03$, Figure 3(d)). In contrast, the myeloid parent population ($p = 0.02$; Figure 3(c)) and macrophage populations ($p = 0.02$) were significantly underrepresented within stroke intracranial blood, with systemic profiles not different compared to CVD controls. Granulocytes in the intracranial blood, though highly susceptible to cell death during processing, trended toward a decrease but were not statistically significant ($p = 0.08$). No other cell populations identified through tSNE were significantly different between intracranial and systemic blood, nor were any parent populations (e.g. B cells, NK cells, or dendritic cells).

We next compared the intracranial and systemic samples from thrombectomy patients to within-patient demographics, including body mass index (BMI), NIHSS on admission, time from last known normal (LKN), and infarct and edema volumes calculated as standard of care. Using Spearman's correlation matrix (Supplemental Figures 9, 10; Supplemental Excel Spreadsheet), we identified that $CD4^+$ T cells populations increased with increased edema volume in both the systemic blood ($r = 0.60$; $p = 0.034$; Supplemental Figure 11A) and the intracranial blood ($r = 0.54$; $p = 0.06$; Figure 3(f)). Increases in patient BMI associated with elevated systemic NK T cell populations ($r = 0.63$; $p = 0.025$; Figure 3(g)), while classical dendritic cell distributions lowered as time from LKN increased in both the intracranial blood ($r = -0.66$; $p = 0.017$; Supplemental Figure 11B) and the systemic blood ($r = -0.71$; $p = 0.009$; Figure 3(h)). There were not significant correlations with NIHSS at time of admission for either systemic or intracranial populations. We note that our study was designed to detect cell type differences within-patient and not powered to detect changes in a behavioral correlates such as NIHSS, including at later times of recovery. As more samples and follow-up data become available, this methodology may be used to draw such correlations.

Correlation of neutrophils in stroke blood samples and thrombi: We compared the proportion of granulocytes in 8 samples of stroke patient blood with the number of neutrophils in the thrombus of those patients. Despite the decreased granulocyte viability in the blood samples, we found a significant ($F_{1,6} = 6.24$; $p = 0.047$; $r^2 = 0.51$) inverse correlation between granulocytes in the systemic blood of stroke patients and neutrophil counts in the thrombus (Figure 4(a), (b)). No

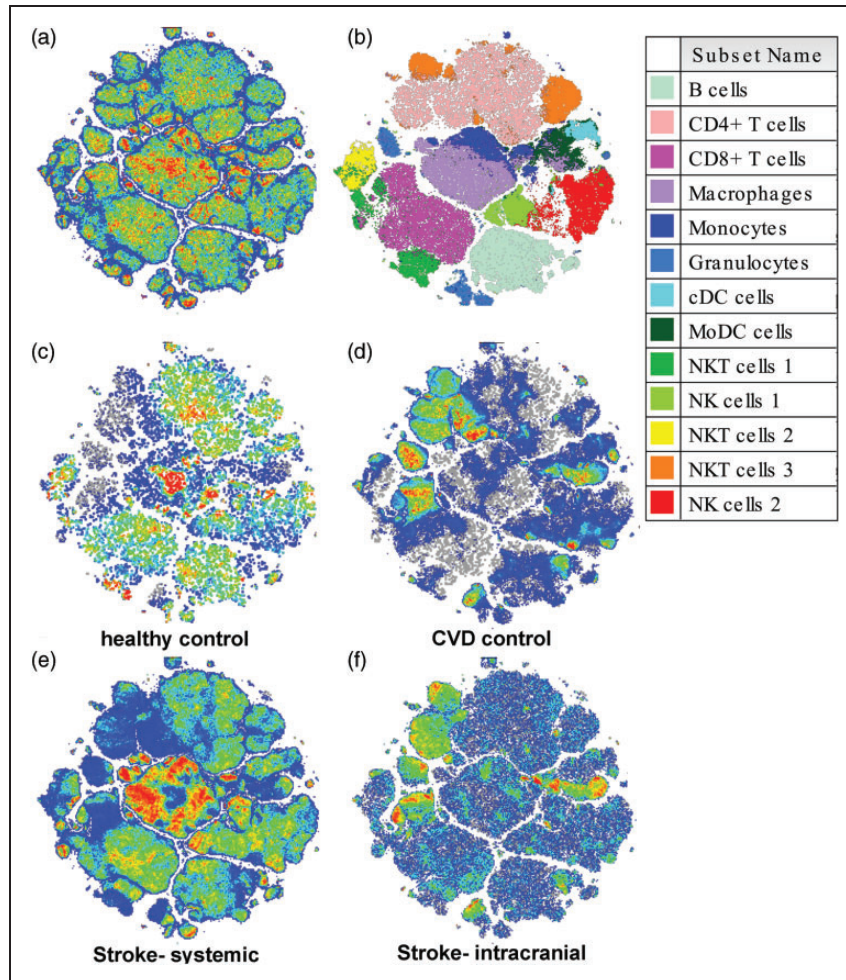


Figure 2. Distribution of tSNE-identified leukocyte populations. (a) tSNE dimensionality reduction and clustering for the general immune panel including innate and adaptive leukocytes. (b) Cell populations identified in A are color coded. (c–f) tSNE overlays of total (grey) and healthy venous control (c), cerebrovascular disease (CVD) control (d), systemic stroke sample (e), and intracranial stroke sample (f). Note the striking differences between systemic and intracranial density localizations, and how they resemble either healthy control or CVD control, respectively.

significant association was found between the intracranial sample and thrombus ($F_{1,6}=0.74$; $p=0.42$; $r^2=0.11$).

Platelets and endothelial cells in intracranial blood samples: A major critique of previous work which established the BACTRAC protocol was the possibility of vessel damage during sample collection, though drawback of blood is standard-of-care to ensure the stent retriever is introduced past the thrombus. But to address this critique, we developed a supplemental panel to measure endothelial cells (CD31), platelets (CD41a), and total leukocytes (CD45) as proportions of live cells (Ghost Dye-negative events). There was no difference in the proportion of platelets between control, intracranial, and systemic blood samples ($F_{2,11}=2.79$, $p=0.10$), as identified as $CD41a^+ CD45^- FSC-A^{low}$ events (Figure 4(c)).

Of the 14 patient samples included in the supplemental panel analysis, only three had a $CD31^+ CD45^-$ endothelial cell proportions greater than 1%: Patients 103, 112, and 114 (Figure 4(d)). The live cell gate of Patient 114 had only 62 total events, which likely skewed the $CD31^+$ endothelial population higher than actuality (to 8%; data not shown). A paired Wilcoxon test on the percent $CD31^+ CD45^-$ cells in systemic vs. intracranial blood, including these outliers, was not significant ($p=0.18$). Patients 112 and 103 did, however, exhibit a substantial (i.e. >10%) and seemingly non-artifactual $CD31^+$ endothelial cell population (Figure 4(e), (f); Case Reports, Supplemental Figures 12, 13). Of note, Patient 112 presenting with the highest $CD31^+$ endothelial cell population showed a hypertensity near the occlusion site and 6mm mid-line shift indicating hemorrhagic transformation, with

Table 2. Circulating leukocyte populations.

	Healthy venous	CVD patients	Stroke arterial		p, Systemic vs. Intracranial
	9.0 mL	Cerebral artery	Systemic	Intracranial	
B cells	13.15 ± 3.92%	7.90 ± 2.98%	10.09 ± 6.20%	9.13 ± 8.81%	0.38
T cells	51.59 ± 6.92%	58.36 ± 14.35%	44.35 ± 17.03%	51.53 ± 18.72%	0.01
CD4+	23.22 ± 5.52%	31.49 ± 12.37%	17.99 ± 7.82%	21.30 ± 8.26%	0.02
CD8+	14.36 ± 6.51%	10.48 ± 4.55%	12.12 ± 6.89%	15.09 ± 8.04%	0.02
Myeloid	14.96 ± 5.88%	15.58 ± 6.93%	24.72 ± 15.27%	18.46 ± 12.16%	0.02
Monocytes	2.19 ± 1.21%	5.10 ± 3.51%	5.06 ± 4.50%	5.24 ± 5.50%	0.86
Macrophages	10.77 ± 4.60%	9.81 ± 4.09%	16.98 ± 11.58%	11.94 ± 8.50%	0.02
Granulocytes	1.01 ± 2.25%	0.42 ± 0.35%	1.89 ± 2.29%	0.85 ± 0.76%	0.08
Dendritic cells	1.76 ± 0.68%	2.72 ± 1.68%	1.94 ± 1.15%	2.26 ± 2.89%	0.63
Classical	0.52 ± 0.25%	0.32 ± 0.16%	0.16 ± 0.14%	0.23 ± 0.39%	0.50
Myeloid	1.24 ± 0.51%	2.40 ± 1.65%	1.78 ± 1.13%	2.04 ± 2.76%	0.63
NK cells	23.39 ± 5.76%	12.43 ± 4.05%	14.37 ± 6.60%	15.51 ± 6.94%	0.41
NKT CD8+ CD3+	2.56 ± 0.89%	1.51 ± 1.83%	2.65 ± 3.30%	3.44 ± 3.34%	0.32
NK CD8+ CD3−	4.39 ± 2.13%	0.94 ± 0.51%	1.47 ± 1.39%	1.40 ± 1.25%	0.35
NKT CD3+	4.82 ± 1.35%	0.79 ± 0.95%	0.66 ± 0.82%	0.65 ± 0.62%	0.67
NKT CD4+ CD3+	3.10 ± 1.65%	5.93 ± 3.33%	3.58 ± 2.73%	4.22 ± 3.18%	0.03
NK	8.53 ± 3.55%	3.25 ± 2.15%	4.88 ± 3.02%	4.59 ± 3.49%	0.71

a 19 mm midline shift at 6 days post-thrombectomy (Figure 4(g)). Despite these 2 patient outliers, endothelial cell proportion was not related to time from LKN ($p = 0.3997$; $r^2 = 0.08$), nor were either platelet or endothelial cell proportions associated with other patient parameters. These samples were all taken prior to initiation of first-pass thrombectomy, so device type and number of passes did not affect results.

Discussion

The post-stroke immune response is complex, involving both pro- and anti-inflammatory mechanisms.^{23–25} In addition to acute monocyte, macrophage, and neutrophil activation,²⁶ B and T cells can promote or ameliorate neuropathology, depending on the lymphocyte subset, location, and timing of activation.^{27–32} Most of our understanding of post-stroke neuroinflammation comes from animal models of stroke, with extensive studies using flow cytometry to identify leukocyte subpopulations in the ischemic parenchyma. For the first time, our modifications to the existing BACTRAC protocol provide the opportunity to study changes in local leukocyte subpopulations residing within the ischemic infarct of patients presenting with ELVO. We found that patients with ischemic stroke have a significantly increased population of both helper and cytotoxic T cells, with a concurrent decrease in macrophages within the ischemic intracranial blood compared to within-patient systemic blood. While we do not know the full immunophenotype of these T cell populations, it is possible they have a

significant role in stroke recovery as recent studies have shown T cells in general, and both T regulatory cells (Tregs) and Th1-like Th17 cells, accumulate in peri-infarct region in patients within days³³ and may be prognostic indicators in stroke and other neurological diseases.^{34–38}

We also cannot confirm to where the innate cells on the ischemic side of the thrombus move, but our current hypothesis is that these cells diapedese into the ischemic parenchyma surrounding the collecting vessel, which would support the early work of Gelderblom and colleagues.²⁶ This seminal paper demonstrated an acute recruitment of innate cells, but not lymphocytes, into the ischemic brain following a transient MCA occlusion in mice.²⁶ Obviously the timing of immune cell trafficking may differ from mice, but methods such as these may eventually be used to understand if the temporal dynamics of immune cell recruitment are conserved across species. Further, this is a single snapshot of the immune milieu at the time of thrombectomy; thus, we are currently unable to differentiate intracranial temporal dynamics. Our results do, however, identify differential responses in immune population trafficking, as we see shifts in both innate (decrease of myeloid cells) and adaptive (increase of T cells) immune cells across the thrombus.

Our prior work from BACTRAC identified several differences in physiologic parameters, as well as genomic and proteomic expression, between the ischemic intracranial and systemic blood. First, we found sex-based differences in pH, pCO₂, and K⁺ in the intracranial vs. systemic blood.³⁹ We also identified changes in

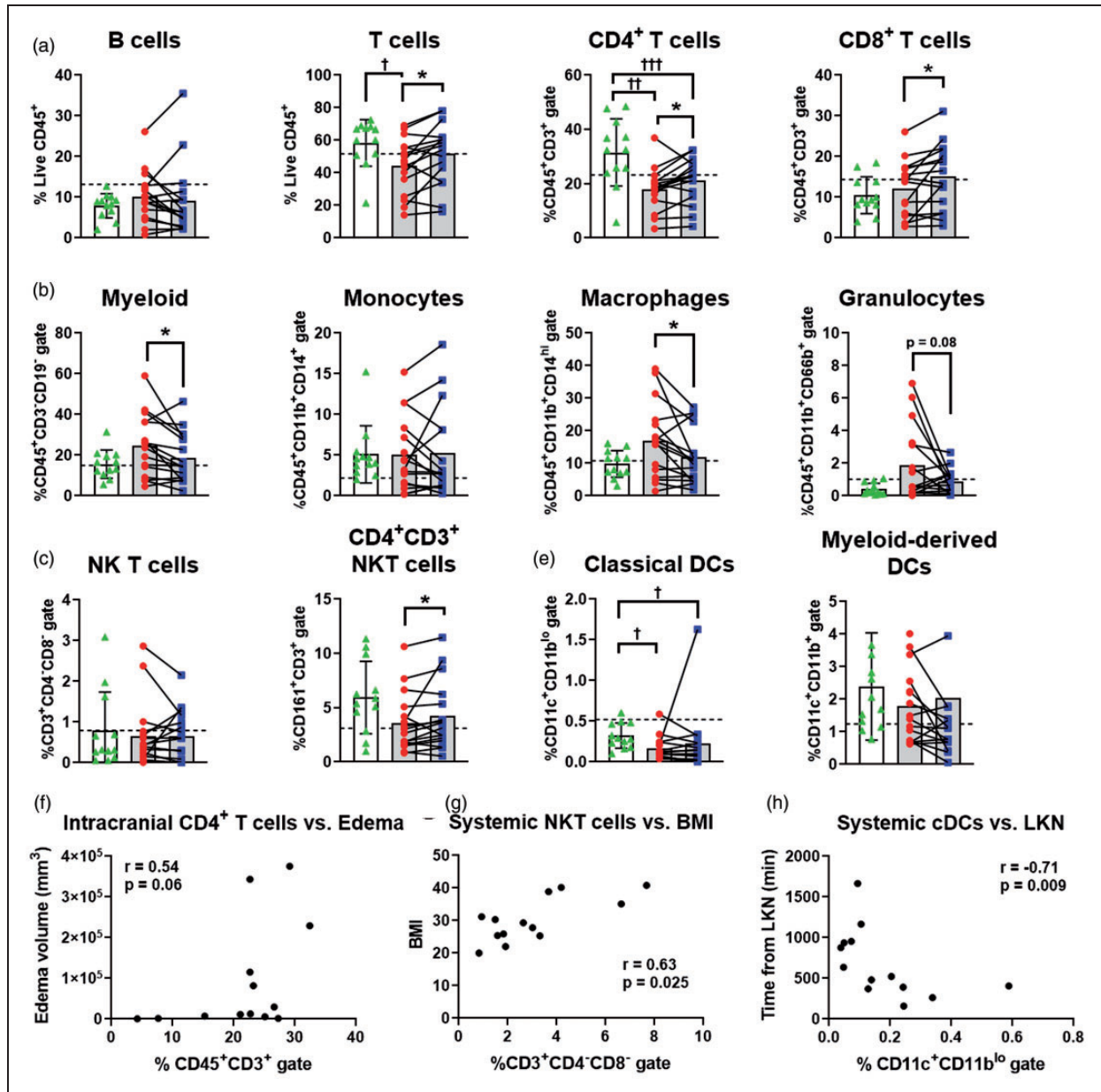


Figure 3. Leukocyte changes in intracranial blood prior to thrombectomy. (a–e) All panels show individual healthy subject control venous populations (dashed line), stroke patient systemic arterial stroke samples (red circles; grey bars), intracranial arterial stroke samples (blue squares; grey bars), and cerebrovascular disease (CVD) control patient samples (green triangles; white bar). Subpopulations for (a) B cells, (b) T cells, (c) innate subpopulations, (d) natural killer (NK) populations, and (e) dendritic cells (DC) are shown as the percent of total live CD45⁺ events and respective subgating on the y axis. *p < 0.05 for within-patient paired t-test; †p < 0.05; ††p < 0.01; †††p < 0.001 from CVD. Control n = 12, stroke n = 16, CVD n = 12. Data also shown as Table 2. (F–H) Results from within-patient Spearman Correlation matrix found association between (f) intracranial CD4⁺ T cells increasing with edema volume, as well as (g) systemic NK T cells increasing with patient BMI, and (h) systemic classical DCs (cDCs) decreasing with time from last known normal (LKN).

base deficit and bicarbonate as predictors of infarct time from LKN, but only in female patients. A separate study used machine learning to identify predictors of injury based on an RNA array of genes associated with inflammatory mechanisms and found specific chemokine and cytokine profiles associated

with infarct volume and edema in ELVO patients.⁴⁰ Thirteen genes in the intracranial blood were identified by machine learning as supporting proliferation of immune cells, in particular Th2 and neutrophil responses. This chemokine/cytokine proliferative response could underlie the elevation of T cell

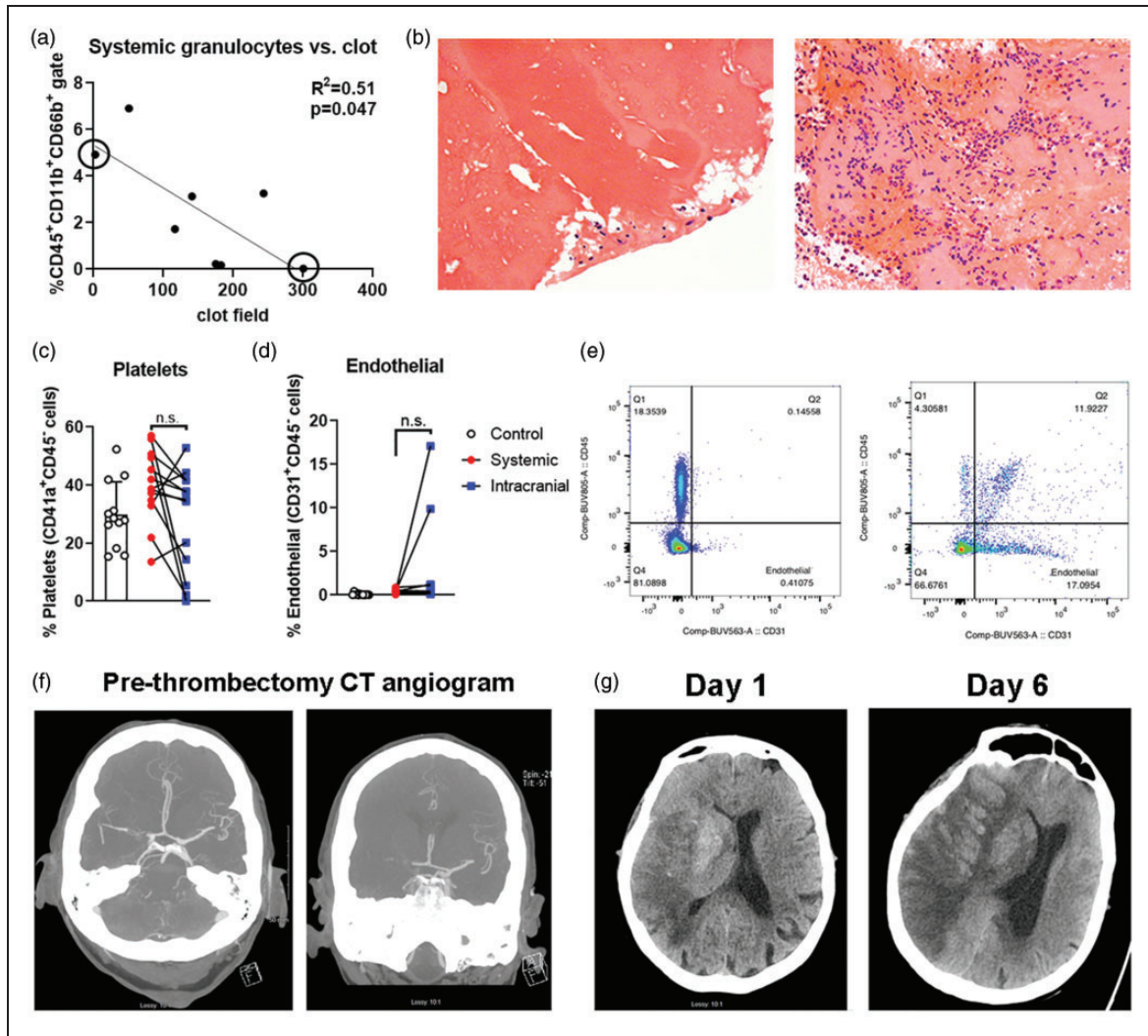


Figure 4. Thrombus, platelet, and endothelial cell analyses. (a) There is a significant inverse correlation between systemic granulocyte populations and neutrophils per clot field. Representative 40X images of (b) thrombus of Patient 99 (left panel; high systemic granulocytes, but low neutrophil count in thrombus) vs. Patient 127 (right panel; low systemic granulocytes, but high neutrophil count in thrombus). (c) Platelet populations are not significantly different between systemic and intracranial samples. Control venous (black circles), systemic arterial stroke samples (red squares) and intracranial arterial stroke samples (blue triangles). (d) Endothelial cell populations are not significantly different between systemic and intracranial samples. (e) Dot plot of systemic CD31 gating (x axes) for systemic and intracranial blood of Patient 112. Note the lack of CD31⁺CD45⁺ events in systemic blood (left panel). Patient 112 shows a substantial CD31⁺CD45⁺ endothelial cell population in intracranial blood (right panel). (f) Patient 112 initial CT angiogram shows vessel occlusion (right panel, black circle). (g) This patient later underwent severe hemorrhagic transformation from Day 1 to Day 6 post-thrombectomy (red ellipse).

populations we identified within the intracranial blood. But based on animal data,²⁶ we would have expected to see a concomitant decline in neutrophil populations (similar to macrophages) as innate cells move into the parenchyma, which we did not find. Significant neutrophil diapedesis could be masked by emergency proliferation, as can occur in bacterial infections in the periphery.⁴¹ Further, the disproportionately high loss of neutrophil viability in both blood samples limits our ability to compare these populations. Therefore, future

studies should use proliferation markers, chemokine, and cytokine analyses in thrombectomy samples to confirm potential immune cell proliferation and activation.

While we did not see significant changes in neutrophil populations in the intracranial blood, a recent study of intracranial blood collected during thrombectomy found a significant increase in leukocyte counts, driven primarily by neutrophils as identified by standard staining of blood smears.⁴² This discrepancy is

likely explained by the short half-life of neutrophils as our collection, isolation, and cryopreservation protocols take 8–12 hours to complete. We did, however, observe a significant inverse correlation between the proportions of neutrophils in the systemic blood to neutrophils in the thrombi. These data suggest that neutrophils may be either invading or becoming trapped in the thrombus. An alternative explanation is that neutrophils are involved in initiating the thrombotic event as has been recently reported in lung thrombi of COVID-19 patients.⁴³ Nonetheless, higher neutrophil counts and lower lymphocyte counts defined patients with poor recovery at 3 months,⁴⁴ highlighting the relevance of identifying leukocyte subpopulations in both the intracranial and systemic blood as potential prognosis of long-term recovery. While our pan-leukocyte panel is limited by poor granulocyte viability, we note that there remain striking differences in the disease-state representation of these cells, a within-patient difference across the thrombus, and significant association between systemic granulocyte proportion and intra-thrombotic neutrophil counts.

We also identified a seemingly true population of live CD31⁺ endothelial cells in the intracranial sample of one patient who later converted to a massive hemorrhagic stroke in the days following thrombectomy. These cells were present only in the intracranial blood, and presumably live based on viability dye. While live endothelial cells can be harvested and cultured from the stent retriever in a swine model of thrombectomy,⁴⁵ we collected the intracranial blood prior to stent placement. Circulating endothelial cells are associated with small vessel vasculitis⁴⁶ and may have been an underlying, albeit undiagnosed, condition in this patient that increased the propensity toward or severity of hemorrhagic transformation.⁴⁷ This would suggest a population already within the circulation and not secondary to either stent-related vascular injury or from within the clot that may be used as a biomarker for risk of hemorrhagic transformation.

In establishing this method, we show that efficient isolation of leukocytes from intracranial blood using the BACTRAC protocol is feasible though limitations remain. We processed volumes as low as 50 μ L with success. These intracranial samples are also of comparable viability to systemic blood processed, even with times from LKN greater than 24 hours. There are, however, significant limitations in the cryopreservation method used, though all within-patient comparisons remain valid as paired samples were frozen and thawed alongside each other. Two phenotypic markers, CXCR3 and CD138, were included in this panel to further identify effector T cells and antibody secreting B cells but we were not able to separate CXCR3⁺ vs. CXCR3⁻ cells clearly and did not identify CD138⁺ events. Further

development of this panel using either spectral flow cytometers, additional markers for immune cell subset quantification, and appropriate dyes or mass cytometry (i.e. CyTOF) would improve the sensitivity and increase the immunophenotyping power.

In summary, this is the first use of flow cytometry in small volume intracranial arterial blood samples of ELVO patients undergoing mechanical thrombectomy. Further, this is also the first demonstration of the BACTRAC protocol to collect and analyze intracranial arterial blood samples from CVD patients undergoing angiography for non-stroke conditions. This provides an unparalleled comparator with respect to the arterial blood samples from stroke patients. While a pilot study with a small sample size, these methods can be used to expand our understanding of acute inflammatory mechanisms activated within the infarcted brain of patients. This novel approach may be critical to identifying immunotherapeutic targets that can be delivered either as adjunctive therapies to mechanical thrombectomy, or in the phases of recovery after stroke.

Funding

The author(s) disclosed receipt of the following financial support for the research, authorship, and/or publication of this article: The project described was supported by the American Heart Association EIA (to AMS), RF1AG059717-01S1, R21AG068370 and F99NS120365 (to BCS), and the National Center for Advancing Translational Sciences, through Grant UL1TR001998 and UKHealthCare. This research was supported by the Biospecimen Procurement & Translational Pathology Shared Resource Facility of the University of Kentucky Markey Cancer Center (P30CA177558). The content is solely the responsibility of the authors and does not necessarily represent the official views of the NIH.

Acknowledgements

We would first like to thank the patients, caregivers, and families for consenting to enrollment in our BACTRAC trial. Finally, we would like to thank Mary Faulkner, Jacque Frank, and Dana Napier for assistance in recruitment, organization, and tissue processing and Dr. Steve Estus for critical discussions.

Declaration of conflicting interests

The author(s) declared no potential conflicts of interest with respect to the research, authorship, and/or publication of this article.


Authors' contributions


TU, JFF, SG, AMS, KRP, and JTC collected patient samples. BCS, GBM, JTC, MG, and AMS designed, optimized, and conducted the experiments. BCS, JTC, MVK, and AMS analyzed the data including histology. GBS, CR, JFF, and AMS analyzed the medical records and compiled the

case report. All authors contributed to manuscript drafts and revisions.

ORCID iDs

Benjamin C Shaw  <https://orcid.org/0000-0001-8862-3840>

Stephen Grupke  <https://orcid.org/0000-0002-7170-6081>

Ann M Stowe  <https://orcid.org/0000-0001-8111-4429>

Supplemental material

Supplemental material for this article is available online.

References

- Fransen PS, Beumer D, Berkhemer OA, et al. MR CLEAN, a multicenter randomized clinical trial of endovascular treatment for acute ischemic stroke in The Netherlands: study protocol for a randomized controlled trial. *Trials* 2014; 15: 343.
- Saver JL, Goyal M, Bonafe A, et al. Solitaire with the intention for thrombectomy as primary endovascular treatment for acute ischemic stroke (SWIFT PRIME) trial: protocol for a randomized, controlled, multicenter study comparing the solitaire revascularization device with IV tPA with IV tPA alone in acute ischemic stroke. *Int J Stroke* 2015; 10: 439–448.
- Campbell BC, Mitchell PJ, Kleinig TJ, et al. Endovascular therapy for ischemic stroke with perfusion-imaging selection. *N Engl J Med* 2015; 372: 1009–1018.
- Jovin TG, Chamorro A, Cobo E, et al. Thrombectomy within 8 hours after symptom onset in ischemic stroke. *N Engl J Med* 2015; 372: 2296–2306.
- Goyal M, Demchuk AM, Menon BK, et al. Randomized assessment of rapid endovascular treatment of ischemic stroke. *N Engl J Med* 2015; 372: 1019–1030.
- Berkhemer OA, Fransen PS, Beumer D, et al. A randomized trial of intraarterial treatment for acute ischemic stroke. *N Engl J Med* 2015; 372: 11–20.
- Nogueira RG, Jadhav AP, Haussen DC, et al. Thrombectomy 6 to 24 hours after stroke with a mismatch between deficit and infarct. *N Engl J Med* 2018; 378: 11–21.
- Malhotra K, Gornbein J and Saver JL. Ischemic strokes due to large-vessel occlusions contribute disproportionately to stroke-related dependence and death: a review. *Front Neurol* 2017; 8: 651–19.
- Boeckh-Behrens T, Kleine JF, Zimmer C, et al. Thrombus histology suggests cardioembolic cause in cryptogenic stroke. *Stroke* 2016; 47: 1864–1871.
- Boeckh-Behrens T, Schubert M, Forschler A, et al. The impact of histological clot composition in embolic stroke. *Clin Neuroradiol* 2016; 26: 189–197.
- Almekhlafi MA, Hu WY, Hill MD, et al. Calcification and endothelialization of thrombi in acute stroke. *Ann Neurol* 2008; 64: 344–348.
- Liebeskind DS, Sanossian N, Yong WH, et al. CT and MRI early vessel signs reflect clot composition in acute stroke. *Stroke* 2011; 42: 1237–1243.
- Marder VJ, Chute DJ, Starkman S, et al. Analysis of thrombi retrieved from cerebral arteries of patients with acute ischemic stroke. *Stroke* 2006; 37: 2086–2093.
- Simons N, Mitchell P, Dowling R, et al. Thrombus composition in acute ischemic stroke: a histopathological study of thrombus extracted by endovascular retrieval. *J Neuroradiol* 2015; 42: 86–92.
- Hashimoto T, Hayakawa M, Funatsu N, et al. Histopathologic analysis of retrieved thrombi associated with successful reperfusion after acute stroke thrombectomy. *Stroke* 2016; 47: 3035–3037.
- Fraser JF, Collier LA, Gorman AA, et al. The Blood And Clot Thrombectomy Registry And Collaboration (BACTRAC) protocol: novel method for evaluating human stroke. *J Neurointerv Surg* 2019; 11: 265–270.
- Martha SR, Fraser JF and Pennypacker KR. Acid-Base and electrolyte changes drive early pathology in ischemic stroke. *Neuromolecular Med*. Epub ahead of print 8 July 2019. DOI: 10.1007/s12017-019-08555-5.
- Martha SR, Cheng Q, Fraser JF, et al. Expression of Cytokines and Chemokines as Predictors of Stroke Outcomes in Acute Ischemic Stroke. *Front Neurol* 2020; 10: 1391. doi: 10.3389/fneur.2019.01391
- Maglinger B, Frank JA, McLouth CJ, et al. Proteomic changes in intracranial blood during human ischemic stroke. *J Neurointerv Surg*. Epub ahead of print 8 July 2020. DOI: 10.1136/neurintsurg-2020-016118.
- Maglinger B, Sands M, Frank JA, et al. Intracranial VCAM1 at time of mechanical thrombectomy predicts ischemic stroke severity. *J Neuroinflammation* 2021; 18: 109.
- Ortega SB, Pandiyan P, Windsor J, et al. A pilot study identifying brain-targeting adaptive immunity in pediatric extracorporeal membrane oxygenation patients with acquired brain injury. *Crit Care Med* 2019; 47: e206–e213.
- Monaco G, Chen H, Poidinger M, et al. flowAI: automatic and interactive anomaly discerning tools for flow cytometry data. *Bioinformatics* 2016; 32: 2473–2480.
- Chamorro A, Meisel A, Planas AM, et al. The immunology of acute stroke. *Nat Rev Neurol* 2012; 8: 401–410.
- Iadecola C, and Anrather J. The immunology of stroke: from mechanisms to translation. *Nat Med* 2011; 17: 796–808.
- Macrez R, Ali C, Toutirais O, et al. Stroke and the immune system: from pathophysiology to new therapeutic strategies. *Lancet Neurol* 2011; 10: 471–480.
- Gelderblom M, Leypoldt F, Steinbach K, et al. Temporal and spatial dynamics of cerebral immune cell accumulation in stroke. *Stroke* 2009; 40: 1849–1857.
- Wang J, Xie L, Yang C, et al. Activated regulatory T cell regulates neural stem cell proliferation in the subventricular zone of normal and ischemic mouse brain through interleukin 10. *Front Cell Neurosci* 2015; 9: 361.
- Ritzel RM, Crapser J, Patel AR, et al. Age-associated resident memory CD8 T cells in the Central nervous system are primed to potentiate inflammation after ischemic brain injury. *J Immunol* 2016; 196: 3318–3330.

29. Liesz A, Zhou W, Mracsko E, et al. Inhibition of lymphocyte trafficking shields the brain against deleterious neuroinflammation after stroke. *Brain* 2011; 134: 704–720.
30. Shichita T, Sugiyama Y, Ooboshi H, et al. Pivotal role of cerebral interleukin-17-producing gammadeltaT cells in the delayed phase of ischemic brain injury. *Nat Med* 2009; 15: 946–950.
31. Bodhankar S, Chen Y, Vandenbark AA, et al. IL-10-producing B-cells limit CNS inflammation and infarct volume in experimental stroke. *Metab Brain Dis* 2013; 28: 375–386.
32. Ortega SB, Torres VO, Latchney SE, et al. B cells migrate into remote brain areas and support neurogenesis and functional recovery after focal stroke in mice. *Proc Natl Acad Sci U S A* 2020; 117: 4983–4993.
33. Heindl S, Ricci A, Carofiglio O, et al. Chronic T cell proliferation in brains after stroke could interfere with the efficacy of immunotherapies. *J Exp Med* 2021; 218: 218: e20202411. doi: <https://doi.org/10.1084/jem.20202411>.
34. Li S, Huang Y, Liu Y, et al. Change and predictive ability of circulating immunoregulatory lymphocytes in long-term outcomes of acute ischemic stroke. *J Cereb Blood Flow Metab*. Epub ahead of print 2 March 2021. DOI: 10.1177/0271678X21995694.
35. Mansilla MJ, Navarro-Barriuso J, Presas-Rodriguez S, et al. Optimal response to dimethyl fumarate is mediated by a reduction of Th1-like Th17 cells after 3 months of treatment. *CNS Neurosci Ther* 2019; 25: 995–1005.
36. Neal EG, Acosta SA, Kaneko Y, et al. Regulatory T-cells within bone marrow-derived stem cells actively confer immunomodulatory and neuroprotective effects against stroke. *J Cereb Blood Flow Metab* 2019; 39: 1750–1758.
37. Stubbe T, Ebner F, Richter D, et al. Regulatory T cells accumulate and proliferate in the ischemic hemisphere for up to 30 days after MCAO. *J Cereb Blood Flow Metab* 2013; 33: 37–47.
38. Xie L, Li W, Hersh J, et al. Experimental ischemic stroke induces long-term T cell activation in the brain. *J Cereb Blood Flow Metab* 2019; 39: 2268–2276.
39. Martha SR, Collier LA, Davis SM, et al. Evaluation of sex differences in acid/base and electrolyte concentrations in acute large vessel stroke. *Exp Neurol* 2020; 323: 113078.
40. Martha SR, Cheng Q, Fraser JF, et al. Expression of cytokines and chemokines as predictors of stroke outcomes in acute ischemic stroke. *Front Neurol* 2019; 10: 1391.
41. Deniset JF, Surewaard BG, Lee WY, et al. Splenic Ly6G (high) mature and Ly6G(int) immature neutrophils contribute to eradication of *S. pneumoniae*. *J Exp Med* 2017; 214: 1333–1350.
42. Kollikowski AM, Schuhmann MK, Nieswandt B, et al. Local leukocyte invasion during hyperacute human ischemic stroke. *Ann Neurol* 2020; 87: 466–479.
43. Zuo Y, Estes SK, Ali RA, et al. Prothrombotic autoantibodies in serum from patients hospitalized with COVID-19. *Sci Transl Med* 2020; 12: eabd3876.
44. Semerano A, Laredo C, Zhao Y, et al. Leukocytes, collateral circulation, and reperfusion in ischemic stroke patients treated with mechanical thrombectomy. *Stroke* 2019; 50: 3456–3464.
45. Jaff N, Grankvist R, Muhl L, et al. Transcriptomic analysis of the harvested endothelial cells in a swine model of mechanical thrombectomy. *Neuroradiology* 2018; 60: 759–768.
46. Woywodt A, Streiber F, de Groot K, et al. Circulating endothelial cells as markers for ANCA-associated small-vessel vasculitis. *Lancet* 2003; 361: 206–210.
47. Boulouis G, de Boysson H, Zuber M, et al. Primary angiitis of the central nervous system: magnetic resonance imaging spectrum of parenchymal, meningeal, and vascular lesions at baseline. *Stroke* 2017; 48: 1248–1255.